



Contents lists available at ScienceDirect

# Journal of Quantitative Spectroscopy & Radiative Transfer

journal homepage: [www.elsevier.com/locate/jqsrt](http://www.elsevier.com/locate/jqsrt)

## Manufactured solutions for the $P_1$ radiation-hydrodynamics equations

Ryan G. McClarren\*, Robert B. Lowrie

Computational Physics Group (CCS-2), Los Alamos National Laboratory, PO Box 1663, MS D413, Los Alamos, NM 87545, USA<sup>1</sup>

## ARTICLE INFO

## Article history:

Received 26 February 2008

Received in revised form

6 June 2008

Accepted 12 June 2008

## Keywords:

Radiation hydrodynamics

Radiative transfer

Hydrodynamics

High-energy density physics

Manufactured solutions

Verification and validation

## ABSTRACT

For the purposes of testing numerical methods, we develop two manufactured solutions to the  $P_1$  radiation-hydrodynamics system. One solution is designed to test numerical methods in the equilibrium diffusion limit, while the other solution is valid in the streaming (small absorption) regime. We then use these solutions to test a discontinuous Galerkin (DG) discretization of the radiation-hydrodynamics system. We demonstrate that DG with linear elements, with either the double minmod slope limiter or no limiter, is second-order accurate and preserves the equilibrium diffusion limit. On the other hand, DG fails to obtain the equilibrium diffusion limit for the step method (i.e., DG with piecewise constant elements), or with linear elements using the minmod limiter. We also show that when the relativistic terms are lagged at the previous time step, the DG method converges at a first-order rate in the streaming regime for both piecewise constant and linear elements.

© 2008 Elsevier Ltd. All rights reserved.

The numerical solution of coupled radiation transport and hydrodynamics presents a challenging unity of two separate fields of computational physics. Computational hydrodynamics and radiation transport each have unique approaches to numerically solving the constituent partial differential equations. For example, radiation transport methods are generally implicit in time to avoid resolving a speed of light based Courant limit, while explicit schemes dominate the compressible hydrodynamics landscape. Moreover, the physical regimes for the different physical processes can be rather dissimilar. Radiation travels at the speed of light while the hydrodynamic flow can be characterized by a sound speed that is, at least for terrestrial applications, many orders of magnitude slower than the speed of light. This separation of scales is especially vexing because in many problems of practical interest, the important features evolve on the hydrodynamic time scale. For example, in an inertial confinement fusion simulation, the ignition of the fuel pellet is initiated by radiatively driven shocks; to get the shock dynamics correct it is necessary to accurately treat the much faster time scale of radiation propagation.

To test a numerical method's suitability for problems of radiation-hydrodynamics, one must take into account not only the performance of the hydrodynamics method and the radiation method in isolation, but also should examine the coupling of the methods. The most straightforward way to test the performance on the coupled system would be to use an exact solution to compare with numerical solutions. Exact solutions are readily available for hydrodynamics alone (see, for example, [1–3]) or radiation transport alone (such as the Su–Olson problems [4–7]). Unfortunately, exact solutions for coupled radiation-hydrodynamics are very sparse. Refs. [8,9] describe solutions for planar radiative shocks. These solutions

\* Corresponding author. Tel.: +1 505 665 1397.

E-mail addresses: [ryanmc@lanl.gov](mailto:ryanmc@lanl.gov) (R.G. McClarren), [lowrie@lanl.gov](mailto:lowrie@lanl.gov) (R.B. Lowrie).<sup>1</sup> Los Alamos National Laboratory is operated by Los Alamos National Security, LLC for the US Department of Energy under contract DE-AC52-06NA25396. LA-UR-08-1083.

require the numerical solution of nonlinear ordinary differential equations and their extension beyond simple radiation models is not clear. Moreover, although these solutions test a code's ability to model a shock discontinuity, generally, one will not attain the theoretical error convergence rate of a numerical method whenever discontinuities are present.

Typically, in order to find an exact solution, one postulates the geometry and initial and boundary conditions in such a way that a solution to the mathematical model may be found. Another way to find a solution is to postulate a solution to the system and then determine spatial and temporally varying source terms that yield the postulated solution; this is known as the method of manufactured solutions (MMS). The use of manufactured solutions, as first introduced to the radiation transport community by Lingus [10], is common in code verification for radiation transport codes [11], and MMS has also been used to verify hydrodynamics codes [12,13]. The solutions generated by MMS are powerful for code verification because it is possible to compare a numerical solution to a smooth, closed-form solution for accuracy and convergence purposes. One drawback to MMS is that general time and space dependent source terms must be implemented in the code, which may not have been considered for other applications.

Below we will introduce a common radiation-hydrodynamics model and develop manufactured solutions for that model. The first solution we develop is a solution of the equilibrium diffusion limit of the radiation-hydrodynamics system [14]. This limit arises when the opacity of the material medium is large and absorption/emission of radiation dominates the free streaming of radiation. We desire a manufactured solution that is valid in this limit because it is important that a numerical method for the radiation-hydrodynamics system limit to a valid numerical method for the equilibrium diffusion equations when a radiation mean-free path is not resolved. Such a method is said to be asymptotic preserving, or that the method has a valid diffusion limit [15–20]. With a manufactured solution in hand, we can understand if a method does preserve the equilibrium diffusion limit of the radiation-hydrodynamics system.

We also develop a solution to the radiation-hydrodynamics system in the regime where the radiation is streaming through the material medium with a small amount of absorption. This solution will make it possible to test numerical methods in the case where the radiation and hydrodynamics variables are evolving at disparate time scales. Such a test is useful because in such situations one often desires taking a time step on the hydrodynamics time scale, and this solution will unambiguously reveal the errors in stepping over the radiation time scale.

After developing our solutions we compare our manufactured solutions with those from a previously published numerical method for the  $P_1$  radiation-hydrodynamics system [21]. The method is based on a semi-implicit, discontinuous Galerkin (DG) finite element treatment of the equations where the source terms are treated implicitly while the advection terms are updated explicitly. We show that the numerical method is asymptotic preserving when linear finite elements are used with either no slope limiter or the double minmod limiter. As expected from previous studies on the uncoupled radiation transport problem [15,16,22], the method fails in the diffusion limit when piecewise constant finite elements, or the minmod limiter with linear elements, is used. Results for the streaming solution converge at first order to the manufactured solution for either piecewise constant or linear finite elements. We conclude that the piecewise linear elements fail to converge at a second-order rate due to the fact that the relativistic terms are lagged at the previous time step.

## 1. Radiation-hydrodynamics model

We will develop solutions to a one-dimensional radiation-hydrodynamics model consisting of the nonrelativistic Euler equations coupled to the grey- $P_1$  radiation transport equations in the absence of scattering. In nondimensional form this model can be expressed as [14]

$$\partial_t \mathbf{u} + \partial_x \mathbf{f}(\mathbf{u}) = \mathbf{s}(\mathbf{u}) + \mathbf{q}, \quad (1a)$$

where

$$\mathbf{u} = \begin{pmatrix} \rho \\ \rho v \\ \rho E \\ E_r \\ F_r \end{pmatrix}, \quad \mathbf{f}(\mathbf{u}) = \begin{pmatrix} \rho v \\ \rho v^2 + p \\ (\rho E + p)v \\ \mathbb{C} F_r \\ \frac{1}{3} \mathbb{C} E_r \end{pmatrix}, \quad \mathbf{s}(\mathbf{u}) = \begin{pmatrix} 0 \\ -\mathbb{P} S_F \\ -\mathbb{P} S_E \\ S_E \\ \mathbb{C} S_F \end{pmatrix}, \quad \mathbf{q} = \begin{pmatrix} Q_\rho \\ Q_v \\ Q_E \\ Q_{E_r} \\ Q_{F_r} \end{pmatrix}. \quad (1b)$$

In the above equations  $\rho$  is the material density,  $v$  the velocity,  $p$  the material pressure, and  $E$  the total internal energy of the material. The radiation energy density is denoted by  $E_r$  and the radiation flux (the first moment of the specific intensity of radiation w.r.t. polar angle) is  $F_r$ . We have also defined

$$S_E = \mathbb{C} \sigma \Phi + \sigma v F_{r_0}, \quad (1c)$$

$$S_F = -\sigma F_{r_0} + \sigma \frac{v}{\mathbb{C}} \Phi, \quad (1d)$$

$$\Phi = T^4 - E_r, \quad (1e)$$

$$F_{r_0} = F_r - \frac{4}{3} \frac{v}{\mathbb{C}} E_r, \quad (1f)$$

with  $T$  the material temperature. The nondimensional parameters are

$$\mathbb{P} = \frac{a_r T_\infty^4}{\rho_\infty a_\infty^2}, \quad \mathbb{C} = \frac{c}{a_\infty}, \quad (2)$$

where  $a_r$  is the radiation constant,  $c$  is the speed of light, and  $a_\infty$  is the reference sound speed at the reference temperature,  $T_\infty$ , and reference density,  $\rho_\infty$ . The parameter  $\mathbb{P}$  is roughly the ratio of radiation pressure to material pressure (or ratio of energies), and is an indicator of the degree to which the hydrodynamics is affected by the radiation field. When  $\mathbb{P}$  is  $O(1)$  or larger, radiation has a significant effect on the dynamics of the material; as  $\mathbb{P} \rightarrow 0$  the material evolution decouples from the evolution of the radiation. Whenever  $\mathbb{P}$  is  $O(1)$ , the physics is well within the so-called high energy density physics regime [23] that can arise in ICF and astrophysics applications.

The parameter  $\mathbb{C}$  is a nondimensional speed of light. For the system (1b) to be valid,  $\mathbb{C}$  must be large, which results in a degree of stiffness, in that streaming radiation propagates at a speed that is  $O(\mathbb{C})$ , whereas the hydrodynamics propagates at  $O(1)$  speeds. Additional stiffness is also the result of the wide range of values that  $\sigma$  may attain, from near-vacuum conditions ( $\sigma \rightarrow 0$ ) to extremely large values in dense materials, such as in the core of a collapsing star. The inherent stiffness in the system (1b) means that our manufactured solutions must address different stiffness regimes.

We use a  $\gamma$ -law equation of state to close the system,

$$E = \frac{p}{\rho(\gamma - 1)} + \frac{1}{2}v^2, \quad (3a)$$

and

$$T = \frac{\gamma p}{\rho}. \quad (3b)$$

The specification of the source vector  $\mathbf{q} = \mathbf{q}(x, t)$  is problem dependent. We use this flexibility in the next section in order to derive an exact solution to the system (1).

The  $P_1$ -Euler model given by (1) is an adequate description of radiation-hydrodynamics in a system where the angular variation in the radiation intensity is weak and the hydrodynamics are inviscid. This is the case in the diffusive radiating shock solutions of Lowrie and Rauenzahn [8] and Lowrie and Edwards [9]. The  $P_1$  radiation model is not adequate for problems with severely anisotropic radiation fields. In this case a higher-order transport model must be used, though the coupling between the material and radiation is analogous to that in (1), that is, radiation interacts with the material through energy and momentum deposition ( $S_E$  and  $S_F$ , respectively).

## 2. Manufactured solutions to the radiation-hydrodynamics system

To develop manufactured solutions to the system (1), we derive the source vector  $\mathbf{q}(x, t)$  such that a given vector  $\mathbf{u}(x, t)$  is a solution of the system (1). The procedure is straightforward: We postulate a solution vector  $\mathbf{u}(x, t)$  and substitute it into the system (1), which then results an explicit expression for  $\mathbf{q}(x, t)$ . In this study, we restrict ourselves to periodic boundary conditions, which simplifies the analysis greatly. Future work should consider more general boundary conditions. In the remainder of this section, we will derive two different manufactured solutions.

### 2.1. Diffusive solution

The first solution we present will be a solution that is consistent with the equilibrium diffusion limit [14]. The equilibrium diffusion limit arises in problems where the opacity is large (i.e.,  $O(\varepsilon^{-1})$ , where  $\varepsilon$  is a small, positive parameter) and  $\mathbb{C}$  is  $O(\varepsilon^{-1})$ . In this limit the leading-order solution for the energy density [14] is

$$E_r = T^4, \quad (4)$$

and the leading-order radiation flux is given by

$$F_r = -\frac{1}{3\sigma}\partial_x T^4 + \frac{4}{3}\frac{v}{\mathbb{C}}T^4. \quad (5)$$

To determine these radiation variables we prescribe the hydrodynamics variables to be

$$\rho = A(\sin(Bx - Ct) + 2), \quad (6a)$$

$$v = A(\cos(Bx - Ct) + 2), \quad (6b)$$

$$p = A\alpha(\cos(Bx - Ct) + 2). \quad (6c)$$

Using this solution we can derive the following quantities through the equation of state:

$$T = \frac{\alpha\gamma(\cos(Bx - Ct) + 2)}{\sin(Bx - Ct) + 2}, \quad (6d)$$

$$E = \frac{A^2}{2} (\cos(Bx - Ct) + 2)^2 + \frac{\alpha(\cos(Bx - Ct) + 2)}{(\gamma - 1)(\sin(Bx - Ct) + 2)}. \quad (6e)$$

The relations (4) and (5) for the radiation variables yield

$$E_r = \frac{\alpha^4 \gamma^4 (\cos(Bx - Ct) + 2)^4}{(\sin(Bx - Ct) + 2)^4}, \quad (6f)$$

$$F_r = \frac{4A\alpha^4 \gamma^4 (\cos(Bx - Ct) + 2)^5}{3\mathbb{C}(2 - \sin(Ct - Bx))^4} - \frac{4B\alpha^4 \gamma^4 (\cos(Bx - Ct) + 2)^3 \sin(Ct - Bx)}{3\sigma(2 - \sin(Ct - Bx))^4} - \frac{4B\alpha^4 \gamma^4 \cos(Bx - Ct)(\cos(Bx - Ct) + 2)^4}{3\sigma(2 - \sin(Ct - Bx))^5}. \quad (6g)$$

The solution given by Eqs. (6) is plotted in Figs. 1–3. These plots take  $A = B = C = 1$ ,  $\alpha = 0.5$ ,  $\gamma = \frac{5}{3}$ , and  $\mathbb{C} = \sigma = 1000$ . The solutions for the radiation variables are plotted at two different times because the temporal behavior of these solutions is not, at first glance, as abecedarian as that of the hydrodynamic variables. We note that the value of the  $F_r$  is small as predicted by the asymptotics of the radiation equations in the diffusive limit.

After substituting the prescribed solutions above into (1), we can then solve for  $\mathbf{q}(x, t)$ . Its components are given by

$$Q_\rho = A(AB \cos(2Ct - 2Bx) + (2AB - C) \cos(Ct - Bx) + 2AB \sin(Ct - Bx)), \quad (7a)$$

$$Q_v = \frac{4B\mathbb{P}\alpha^4 (\cos(Ct - Bx) + 2)^3 (2 \cos(Ct - Bx) - 2 \sin(Ct - Bx) + 1) \gamma^4}{3(\sin(Ct - Bx) - 2)^5} + A^3 B \cos(Ct - Bx) (\cos(Ct - Bx) + 2)^2 - A^2 C \cos(Ct - Bx) (\cos(Ct - Bx) + 2) + AB\alpha \sin(Ct - Bx) + A^2 C (\sin(Ct - Bx) - 2) \sin(Ct - Bx) - 2A^3 B (\cos(Ct - Bx) + 2) (\sin(Ct - Bx) - 2) \sin(Ct - Bx), \quad (7b)$$

$$Q_E = \frac{8AB\mathbb{P}\alpha^4 \gamma^4 (\cos(Ct - Bx) + 2)^4}{3(\sin(Ct - Bx) - 2)^4} - \frac{4AB\mathbb{P}\alpha^4 \gamma^4 (2 \cos(Ct - Bx) - 3) (\cos(Ct - Bx) + 2)^4}{3(\sin(Ct - Bx) - 2)^5} - \frac{A^3}{2} (2AB + A \cos(Ct - Bx) B - 2C) \sin^2(Ct - Bx) (\cos(Ct - Bx) + 2) + \frac{1}{8} A^3 (3AB \cos(3Ct - 3Bx) + 16AB \cos(2Ct - 2Bx) + \cos(Ct - Bx) (17AB - 8C - 4C \cos(Ct - Bx)) + 8AB \sin(2Ct - 2Bx) (\cos(Ct - Bx) + 2) + \frac{A \sin(Ct - Bx)}{\gamma - 1} ((B(\gamma - 1) \cos^2(Ct - Bx) A^3 + 12B(\gamma - 1) A^3 - 4C(\gamma - 1) A^2 + 4B\alpha\gamma A + 2(4B(\gamma - 1) A^2 + (C - C\gamma) A + B\alpha\gamma) \cos(Ct - Bx) A - C\alpha)), \quad (7c)$$

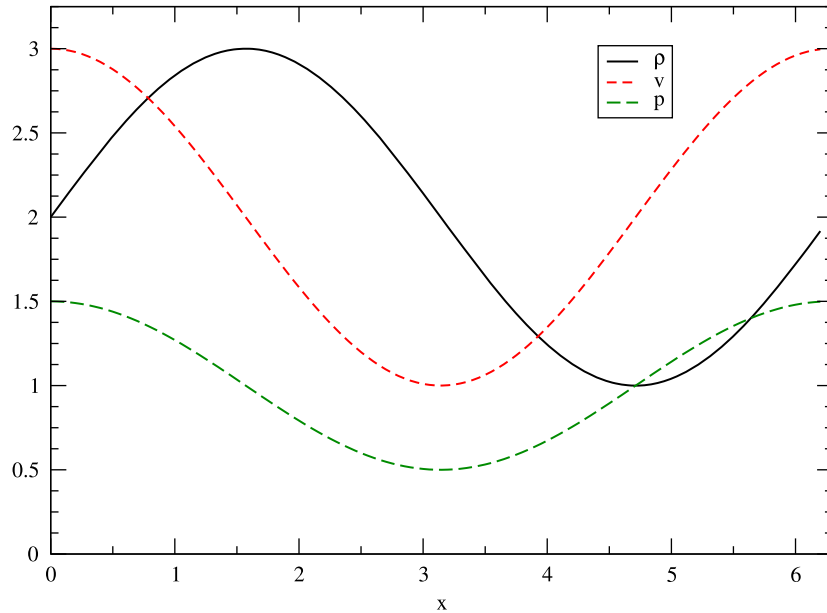
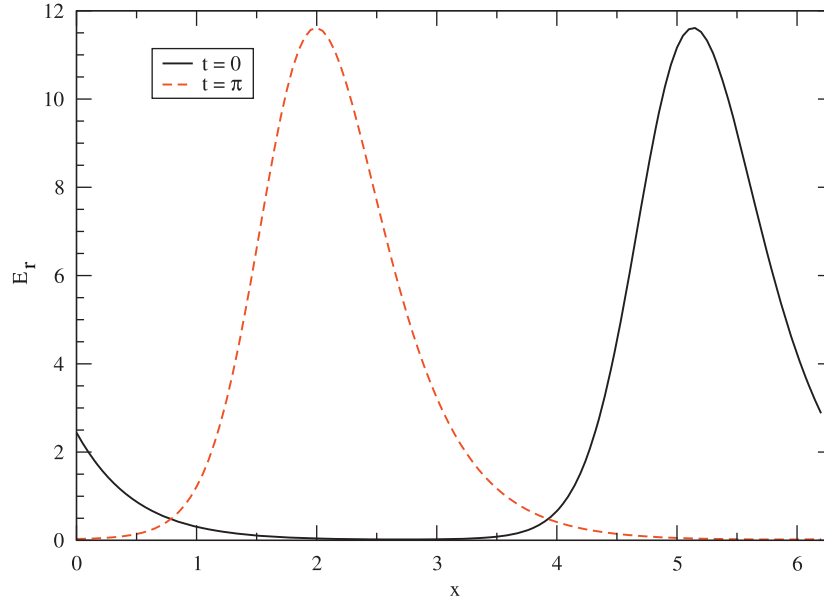
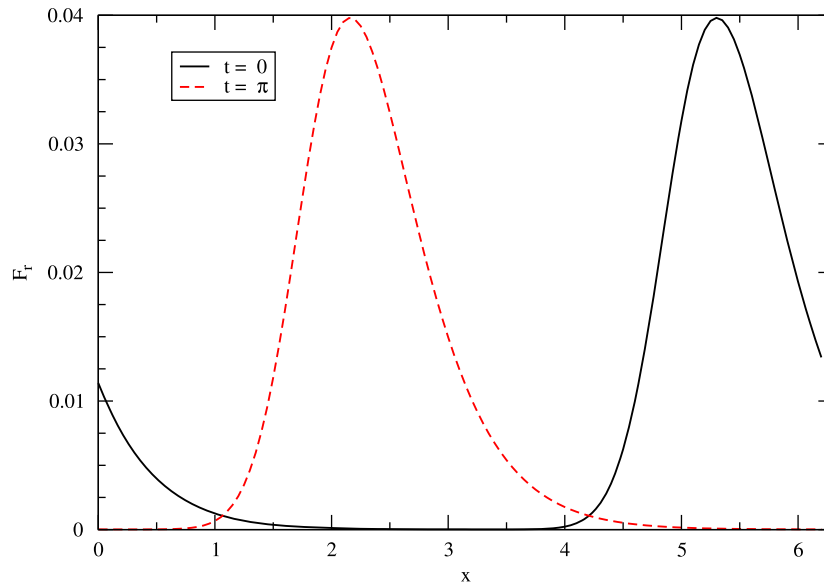


Fig. 1. Diffusion solution for the hydrodynamic variables,  $\rho$ ,  $v$ , and  $p$ , at  $t = 0$ .



**Fig. 2.** Diffusion solution for the radiation energy density,  $E_r$ , at  $t = 0, \pi$ .



**Fig. 3.** Diffusion solution for the radiation flux,  $F_r$ , at  $t = 0, \pi$ .

$$\begin{aligned}
 Q_{E_r} = & \frac{1}{12\sigma(\sin(Ct - Bx) - 2)^6} (\alpha^4 \gamma^4 (\cos(Ct - Bx) + 2)^2 (-320CB^2 - 16C \cos(2Ct - 2Bx)B^2 \\
 & - 184C \cos(Ct - Bx)B^2 + 8C \sin(3Ct - 3Bx)B^2 + 256C \sin(2Ct - 2Bx)B^2 - 1836A\sigma B \\
 & + 28A\sigma \cos(4Ct - 4Bx)B - 272A\sigma \cos(2Ct - 2Bx)B - 2384A\sigma \cos(Ct - Bx)B - A\sigma \sin(5Ct - 5Bx)B \\
 & + 12A\sigma \sin(4Ct - 4Bx)B + 261A\sigma \sin(3Ct - 3Bx)B + 1304A\sigma \sin(2Ct - 2Bx)B + 384C\sigma \\
 & - 8(CB^2 - 18A\sigma B + 3C\sigma) \cos(3Ct - 3Bx) + 504C\sigma \cos(Ct - Bx) - 24C\sigma \sin(3Ct - 3Bx) \\
 & - 216C\sigma \sin(2Ct - 2Bx) + 2(164CB^2 + 1091A\sigma B - 252C\sigma) \sin(Ct - Bx)), \quad (7d)
 \end{aligned}$$

$$\begin{aligned}
Q_{F_r} = & \frac{1}{12\mathbb{C}\sigma(\sin(\mathbb{C}t - Bx) - 2)^6} (C\alpha^4\gamma^4(\cos(\mathbb{C}t - Bx) + 2)^2(4A\sigma((\sin(3\mathbb{C}t - 3Bx) \\
& - 16\sin(2\mathbb{C}t - 2Bx) - 99\sin(\mathbb{C}t - Bx))(\cos(\mathbb{C}t - Bx) + 2)^2 \\
& - 6\cos(4\mathbb{C}t - 4Bx) - 32\cos(3\mathbb{C}t - 3Bx) + 48\cos(2\mathbb{C}t - 2Bx) + 480\cos(\mathbb{C}t - Bx)) \\
& + 8(40B\mathbb{C} + B(\cos(3\mathbb{C}t - 3Bx) + 2\cos(2\mathbb{C}t - 2Bx) + 23\cos(\mathbb{C}t - Bx) \\
& - \sin(3\mathbb{C}t - 3Bx) - 32\sin(2\mathbb{C}t - 2Bx) - 41\sin(\mathbb{C}t - Bx))\mathbb{C} + 187A\sigma)). \quad (7e)
\end{aligned}$$

With the source vector  $\mathbf{q}(x, t)$  defined by (7), a solution to the radiation-hydrodynamics system (1) is therefore given by Eqs. (6). This solution will allow us to explore the equilibrium diffusion limit of numerical methods that solve the  $P_1$  radiation-hydrodynamics system. Previous work, for example [17,18,20,24], has examined the discretization of the radiation transport operator in this limit. Several reasonable numerical schemes for the radiation transport fail in the diffusion limit when a mean-free path, that is  $1/\sigma$ , is not resolved by the mesh spacing. Other methods, those that are said to be accurate in the diffusion limit, can have thousands of mean-free paths in a single computational cell and converge to the proper diffusion solution. With the manufactured solution above, the behavior of various numerical methods in the equilibrium diffusion limit can be investigated for the coupled system.

The sources given by (7) are plotted in Figs. 4–6 with  $A = B = C = 1$ ,  $\alpha = 0.5$ ,  $\gamma = 5/3$ ,  $\mathbb{C} = \sigma = 1000$ , and  $\mathbb{P} = 0.001$ . We draw the reader's attention to the fact that  $Q_{E_r}$ , our prescribed source for the radiation energy density, is an  $O(1)$  quantity. This is important because of the way we have written the radiation operator in Eq. (1), any sources must be  $O(1)$  to obtain the equilibrium diffusion limit. The source will not be  $O(1)$  if the value of  $\alpha$  were increased. In fact, if  $\alpha = 1$ , the maximum value of  $Q_{E_r}$  is nearly 300. Similarly,  $Q_{F_r}$  must be  $O(\varepsilon)$ , as Fig. 6 reveals that it is, to yield the equilibrium diffusion limit.

The radiation sources in Eqs. (7) are proportional to  $1/\sigma$ . Therefore, this solution is not well suited to testing the thin limit (i.e., when  $\sigma$  is small) of the radiation-hydrodynamics system. If the solution above were implemented with a small value of  $\sigma$ , the prescribed sources would dominate the effects of the numerical treatment of the other terms in the system. To address this issue, in the next section we develop a solution for this thin limit when the radiation streaming dominates absorption.

## 2.2. Streaming solution

In this section we will develop a solution where the radiation and hydrodynamics are weakly coupled, so that the radiation energy travels much faster than fluid energy. This is the case whenever the material is optically thin and the radiation streams through. This solution will be far from the equilibrium-diffusion limit that was considered in the previous section. A separate manufactured solution is needed for this regime because the solution that developed the diffusive solution is inappropriate here, as discussed in the last section.

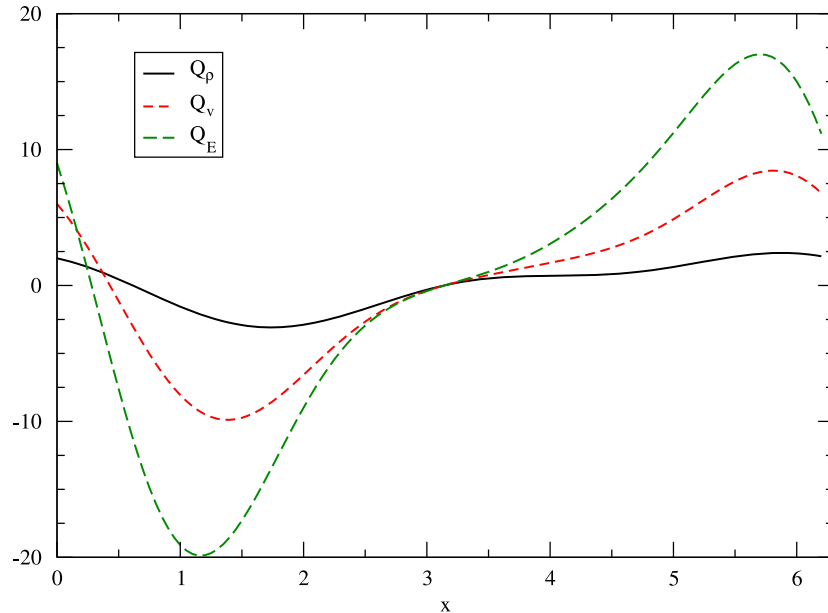
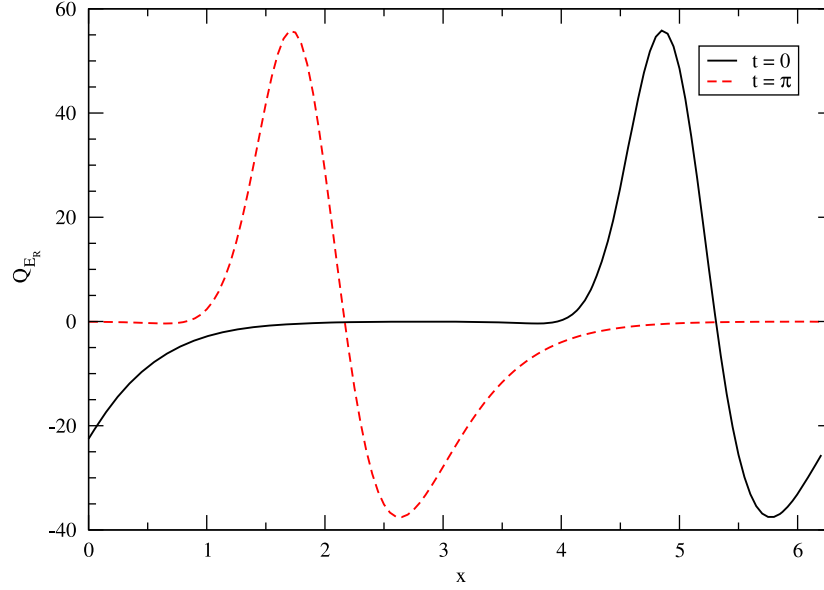
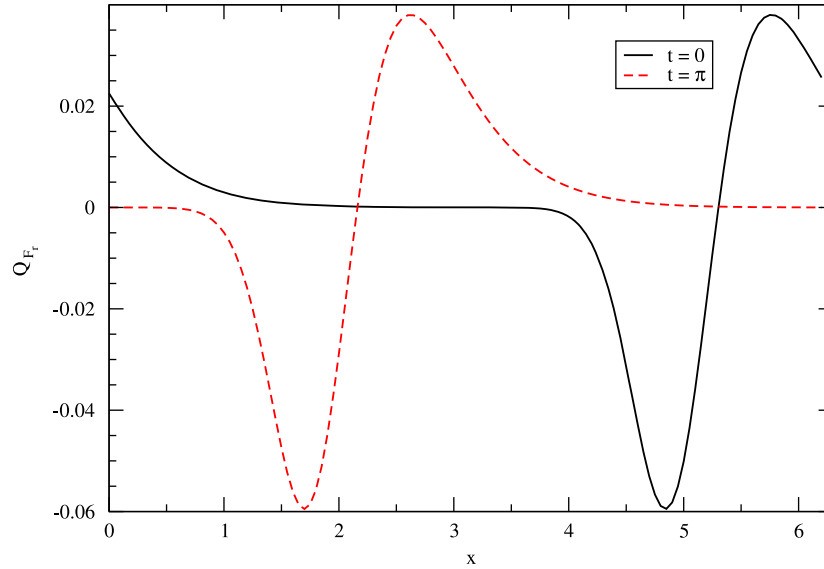


Fig. 4. Hydrodynamic sources,  $Q_\rho$ ,  $Q_v$ , and  $Q_E$ , for the diffusion solution at  $t = 0$ .



**Fig. 5.** Radiation energy source,  $Q_{E_r}$ , for the diffusion solution at  $t = 0, \pi$ .



**Fig. 6.** Radiation flux source,  $Q_{F_r}$ , for the diffusion solution at  $t = 0, \pi$ .

For this case we choose the solution to be

$$\rho = A(\sin(Bx - Ct) + 2), \quad (8a)$$

$$v = \frac{1}{A(\sin(Bx - Ct) + 2)}, \quad (8b)$$

$$p = A\alpha(\sin(Bx - Ct) + 2), \quad (8c)$$

$$E_r = \alpha(\sin(Bx - \mathbb{C}Ct) + 2), \quad (8d)$$

$$F_r = \alpha(\sin(Bx - \mathbb{C}Ct) + 2). \quad (8e)$$

Note that the radiation variables change much more quickly than the hydrodynamic variables. The wave speed of the hydrodynamic variables is given by  $C/B$ , while the wave speed of the radiation variables is  $\mathbb{C}C/B$ . Again, here we are seeking

solutions where the radiation and hydrodynamics are only weakly coupled. Also, note that in dimensional form,  $F_r \approx cE_r$ , which is consistent with a streaming solution.

Using solution (8) we can derive the following quantities through the equation of state:

$$T = \alpha\gamma, \quad (9a)$$

$$E = \frac{\alpha}{\gamma - 1} + \frac{1}{2A^2(\sin(Ct - Bx) - 2)^2}. \quad (9b)$$

That the material temperature is constant is so that we mimic an isothermal flow regime, where the radiation acts on a fast enough time scale that material temperature deviations are suppressed. A dispersion analysis of the radiation-hydrodynamic equations shows that the material acts isothermally for intermediate optical depths; see, for example, Ref. [14].

As before, we substitute this solution into the radiation-hydrodynamics system (1) and solve for  $\mathbf{q}(x, t)$ . We obtain

$$Q_\rho = -AC \cos(Bx - Ct), \quad (10a)$$

$$Q_v = \cos(Ct - Bx) \left( AB\alpha - \frac{B}{A(\sin(Ct - Bx) - 2)^2} \right) + \frac{\mathbb{P}\alpha\sigma(-3\alpha^3\gamma^4 + 12AC + 3AC \sin(Ct - Bx)(\sin(Ct - Bx) - 2) + (1 - 6AC) \sin(Ct - Bx) - 2)}{3AC(\sin(Ct - Bx) - 2)}, \quad (10b)$$

$$Q_E = \frac{1}{12A^2(\sin(Ct - Bx) - 2)^3} \times \left( \frac{1}{\gamma - 1} (6 \cos(Ct - Bx)(C\alpha \cos(2Ct - 2Bx)(\sin(Ct - Bx) - 6)A^3 + C(-25\alpha A^2 + \gamma - 1) \sin(Ct - Bx)A + 2(AC(11\alpha A^2 - \gamma + 1) + B(\gamma - 1)))) \right. \\ \left. + \frac{1}{C} (4\mathbb{P}\alpha\sigma(\sin(Ct - Bx) - 2)(4(3AC(AC(\alpha^3\gamma^4 - 2) + 1) + \sin(Ct - Bx) - 2) + 3AC(\sin(Ct - Bx)(-4AC\alpha^3\gamma^4 + 8AC + AC(\alpha^3\gamma^4 - 2)\sin(Ct - Bx) - 2) \right. \\ \left. + (\sin(Ct - Bx) - 2)(-2AC + A \sin(Ct - Bx)C + 1) \sin(Ct - Bx))) \right), \quad (10c)$$

$$Q_{E_r} = B\mathbb{C}\alpha \cos(Ct - Bx) - C\mathbb{C}\alpha \cos(Ct - Bx) - \mathbb{C}\alpha\sigma(\alpha^3\gamma^4 + \sin(Ct - Bx) - 2) - \frac{\alpha\sigma(-6AC + 3AC \sin(Ct - Bx)C + 4)(\sin(Ct - Bx) - 2)}{3A^2C(\sin(Ct - Bx) - 2)^2}, \quad (10d)$$

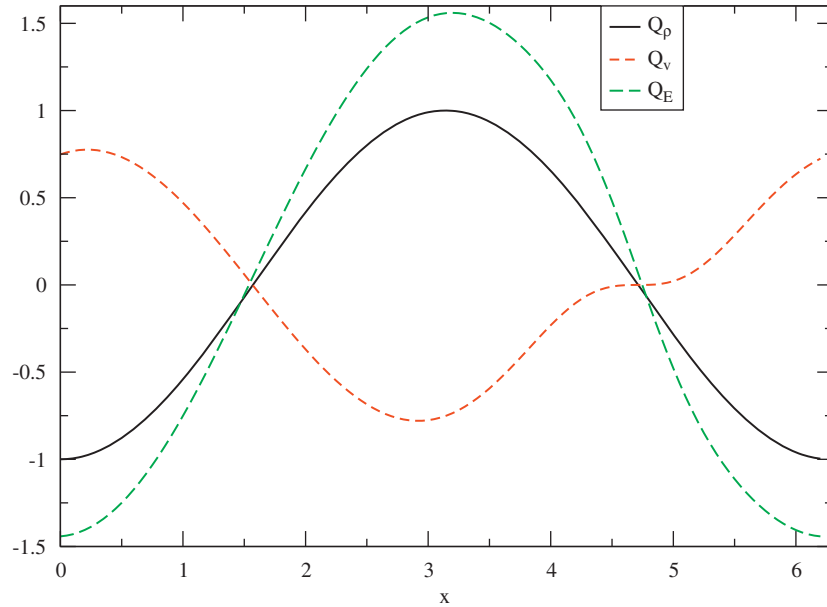


Fig. 7. The hydrodynamic sources,  $Q_\rho$ ,  $Q_v$ , and  $Q_E$ , for the streaming solution at  $t = 0$ .



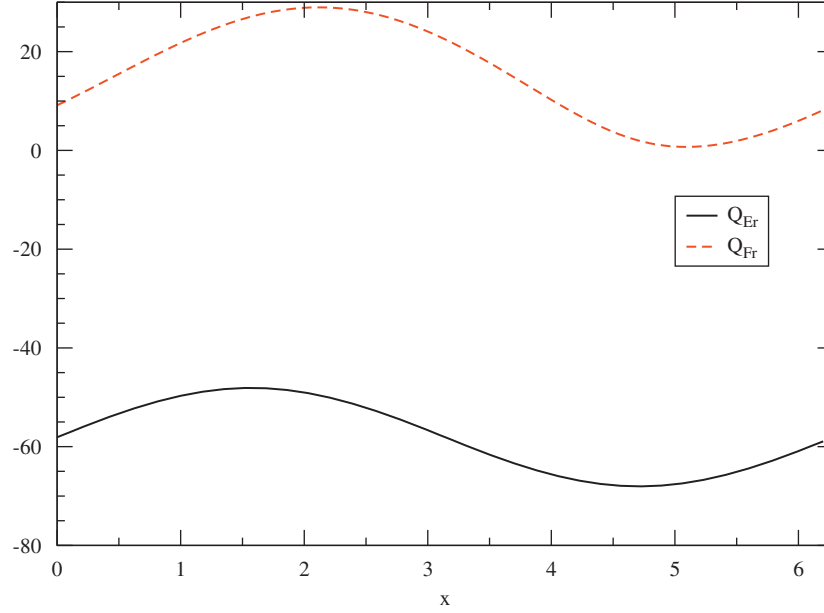


Fig. 8. The radiation energy sources,  $Q_{Er}$  and  $Q_{Fr}$ , for the streaming solution at  $t = 0$ .

$$Q_{Fr} = \frac{1}{3A(\sin(Ct - Bx) - 2)} \times (\alpha(\sigma(3\alpha^3\gamma^4 - 12AC - 3AC\sin(Ct - Bx)(\sin(C\mathbb{C}t - Bx) - 2) + A(B - 3C)\mathbb{C}\cos(C\mathbb{C}t - Bx)(\sin(Ct - Bx) - 2) + (6A\mathbb{C} - 1)\sin(C\mathbb{C}t - Bx) + 2))). \quad (10e)$$

These sources are plotted in Figs. 7 and 8 with  $A = B = C = \alpha = 1$ ,  $\gamma = \frac{5}{3}$ ,  $\mathbb{C} = 10$ ,  $\sigma = 1$ , and  $\mathbb{P} = 0.001$ . Note that the amplitude of each term in the radiation sources is proportional to either the nondimensional speed of light,  $\mathbb{C}$ , or the opacity,  $\sigma$ . Therefore, in the equilibrium diffusion limit, these source terms are  $O(\varepsilon^{-1})$ . This behavior is necessary because Eqs. (8d), (8e) never satisfy Eqs. (4) and (5), even as  $\varepsilon \rightarrow 0$ . The source terms  $Q_{Er}$  and  $Q_{Fr}$  must be  $O(\varepsilon^{-1})$  in order to prevent the solution (8) from attaining the equilibrium diffusion limit. In other words, just as the diffusive manufactured solution is inappropriate in the streaming regime, the streaming manufactured solution is inappropriate in the diffusive regime. Both solutions are needed in order to test a method for radiation hydrodynamics.

### 3. Comparison with numerical methods

Previously, Lowrie and Morel [21] presented a DG method for  $P_1$  radiation-hydrodynamics. Here we will use their scheme on the manufactured solution problems presented above. First, we give a sketch of their numerical method.

The method takes the system (1) and integrates in time using a predictor–corrector scheme:

$$\frac{\mathbf{u}^{n+1/2} - \mathbf{u}^n}{\Delta t/2} + \partial_x \mathbf{f}(\mathbf{u}^n) = \mathbf{s}(\mathbf{u}^{n+1/2}), \quad (11a)$$

$$\frac{\mathbf{u}^{n+1} - \mathbf{u}^n}{\Delta t} + \partial_x \mathbf{f}(\mathbf{u}^{n+1/2}) = \theta \mathbf{s}(\mathbf{u}^{n+1}) + (1 - \theta) \mathbf{s}(\mathbf{u}^n), \quad (11b)$$

for  $0 \leq \theta \leq 1$ , and  $\mathbf{u}^n = \mathbf{u}(x, n\Delta t)$ . This approach treats the streaming term,  $\mathbf{f}(\mathbf{u})$ , explicitly using the second-order Runge–Kutta. The source terms are treated implicitly; when  $\theta = 1$ , these terms are treated using the backward Euler method, whereas,  $\theta = \frac{1}{2}$  gives the Crank–Nicolson method. This type of time integration has been called implicit–explicit (IMEX) time integration or, alternatively, semi-implicit time integration.

The spatial-discretization used by Lowrie and Morel is the DG method [25]. In this method, the solution in a spatial cell,  $k$ , that spans  $[x_{k-1/2}, x_{k+1/2}]$  is given by

$$\mathbf{u}_k(x, t) = \sum_{j=0}^m u_{kj} \phi_m(x), \quad (12)$$

where  $m$  is the degree of the expansion, and the basis set,  $\{\phi\}$ , are the Lagrange–Legendre polynomials. Here we will be interested in the  $m = 0$  and 1 cases. For these cases the basis functions are

$$\phi_0 = 1 \quad \text{for } x \in [x_{k-1/2}, x_{k+1/2}], \quad (13a)$$

$$\phi_1 = \frac{x}{\Delta x} \quad \text{for } x \in [x_{k-1/2}, x_{k+1/2}], \quad (13b)$$

where  $\Delta x = x_{k+1/2} - x_{k-1/2}$ .

For the case of  $m = 0$ , the unknown in each cell is the cell average of  $\mathbf{u}$ . This method is often referred to as the “step method” in the radiation transport literature. The  $m = 1$  case, sometimes called the linear discontinuous (LD) method, has two unknowns per cell: the cell average of  $\mathbf{u}$  and the slope of each element of  $\mathbf{u}$ . For radiation transport the LD method with the predictor–corrector approach has been shown to be second order [26].

The DG method requires the solution of a Riemann problem at each cell interface. For the hydrodynamics variables we use Roe’s approximate Riemann solver [27] for the “frozen” Riemann problem; here, frozen refers to a Riemann problem that ignores the source term when computing the hydrodynamic flux (see Ref. [20] for a detailed discussion). The streaming terms in the radiation transport are linear and the exact frozen Riemann problem can be solved easily.

### 3.1. Equilibrium diffusion results

Previously, analysis has shown that the step method ( $m = 0$ ) fails in the equilibrium diffusion limit for radiation transport problems without hydrodynamics coupling when the radiation mean-free path is not resolved by the mesh spacing [15,18,20]. On the other hand, the LD method ( $m = 1$ ) gives a second-order spatial discretization in the diffusion limit for radiation transport.

Using the diffusive manufactured solution we are in a position to examine if these results extend to the case of radiation-hydrodynamics. We define the resolution of the grid using the parameter

$$\tau = \frac{\Delta x}{\varepsilon}. \quad (14)$$

The parameter  $\tau$  measures the optical thickness of a spatial cell; the case we are interested in has  $\tau \gg 1$ , that is when there are many radiation mean-free paths in each spatial cell.

To determine if a method is accurate in the equilibrium diffusion limit, we measure the solution error at a fixed value of  $\tau$  and a fixed CFL number ( $\text{CFL} = \mathbb{C} \Delta t / \Delta x$ ), while decreasing  $\Delta x$ . By fixing  $\tau$  and varying  $\Delta x$  we are comparing errors at a fixed optical thickness; as the mesh spacing,  $\Delta x$ , is decreased the shape of the solution is better resolved; however, the mean-free path of radiation is not. A method that is accurate in the equilibrium diffusion limit has its error vanish as  $\Delta x \rightarrow 0$  and  $\varepsilon \rightarrow 0$ , for a constant value of  $\tau$ . A method that fails in the equilibrium diffusion limit requires that  $\tau \rightarrow 0$  as  $\varepsilon \rightarrow 0$ , which requires unreasonably small mesh sizes. Note that in order to test the ability of a method to attain this limit, a constant value of  $\tau$  requires us to change the dimensionless values  $\sigma$  and  $\mathbb{C}$  as the mesh is refined.

In Fig. 9 the convergence of  $m = 0$  and 1 finite elements on the diffusive problem with a constant value of  $\tau$ . This problem was run on a computational domain of  $x \in [0, 2\pi]$  and had the source parameters as  $A = B = 1$ ,  $C = 10$ ,  $\alpha = 0.5$ ,  $\gamma = \frac{5}{3}$ ,  $\mathbb{P} = 0.001$ . The opacity and speed of light were set as  $\mathbb{C} = \sigma = 1000N_x/20$  for  $N_x$  equal to the number of cells in the computational domain. We ran the problem until time  $t = 2\pi$ ; that is, until the initial condition has propagated one wavelength. The CFL number used was 0.3 (the stability limit is  $\frac{1}{3}$ ). Also, the  $m = 1$  solutions used the double minmod slope limiter [28]. We quantify the error between the exact solution and the numerical solution using the  $L_2$  norm,

$$L_2(E_r) = \sqrt{\frac{1}{N_x} \sum_{k=1}^{N_x} [E_{r,k} - E_r^{\text{exact}}(k \Delta x)]^2}. \quad (15)$$

We use the radiation energy density as the variable to compare with the exact solution because it is in this variable that we observed the greatest error.

On this problem the  $m = 1$  results converge to the exact solution at a second-order rate, in space and time. This result was expected theoretically; however, this is the first time numerical results have borne this out on the coupled radiation-hydrodynamics system. The fact that the method converges when  $\tau \gg 1$  confirms that this method is accurate in the equilibrium diffusion limit. We also note that the choice of  $\theta$  had very little effect on the error. This suggests that for this problem and range of mesh sizes, the error was dominated by spatial error rather than time integration error. Keep in mind that the diffusion solution evolves on a hydrodynamic time scale, yet our time integration method is restricted by a CFL limit based on  $\mathbb{C}$ . Therefore, the time step is very small so that the overall temporal error is small.

The step method ( $m = 0$ ) did not converge to the exact solution—even when there were 320 mesh cells in the computational domain. Hence, we have demonstrated numerically that this method fails in the equilibrium diffusion limit. This agrees with previous results for the step method in radiation transport problems without hydrodynamic effects [15]. Finally, we note that other numerical results not shown here for the sake of brevity demonstrate that varying the  $\mathbb{P}$  parameter does not change the convergence properties of the method in the diffusion limit.

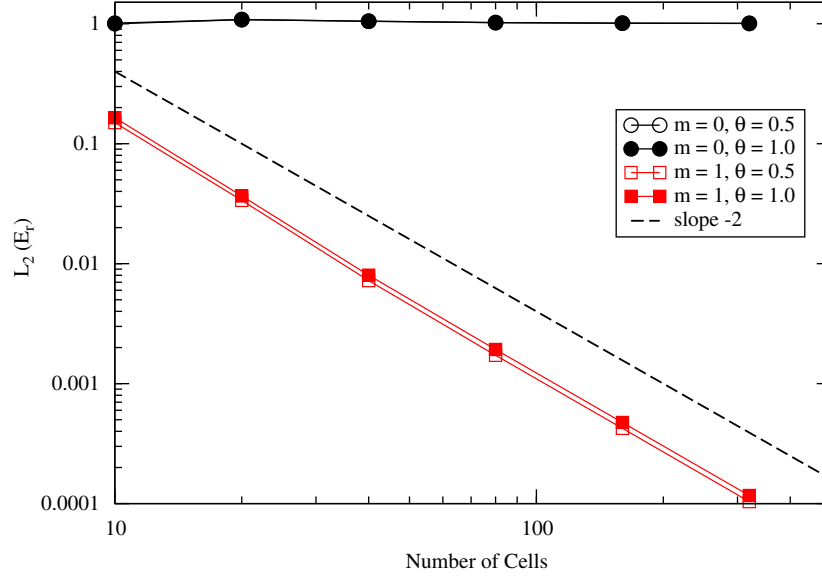


**Fig. 9.** Error between the numerical and analytic solutions for the diffusive manufactured solution for varying number of cells with CFL = 0.3 and  $\tau = 100\pi$ . The  $m = 0$  results, for  $\theta = 0.5$  and  $\theta = 1.0$ , are coincident on this scale. In this problem  $\mathbb{C} = \sigma = 1000N_x/20$ .

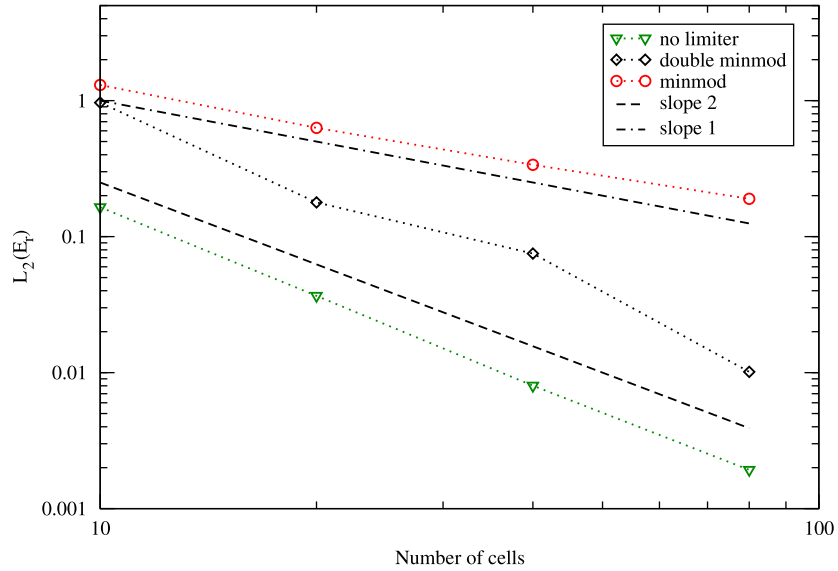


**Fig. 10.** Error between the numerical and analytic solutions for the diffusive manufactured solution for different slope limiters with CFL = 0.3,  $\tau = 100\pi$ , and  $\theta = 1.0$ . In this problem  $\mathbb{C} = \sigma = 1000N_x/20$ .

### 3.1.1. Comparison of slope limiters in the equilibrium diffusion limit

Recently, McClarren and Lowrie demonstrated that though the DG method is asymptotic preserving, certain limiters can cause the method to fail in the equilibrium diffusion limit [22]. They concluded that the double minmod limiter does preserve the equilibrium diffusion limit for pure radiation transport, whereas the minmod limiter does not.

As in our comparison above, we will use the diffusive manufactured solution to determine how different limiters behave in the equilibrium diffusion limit. Unless noted, the solution parameters are set as in the previous section.

Figs. 10 and 11 show the error convergence for the double minmod and minmod slope limiters along with the error from the unlimited solution. In Fig. 10 the minmod limited solution converges at a first-order rate to the manufactured solution. Therefore, when  $\tau = 100\pi$  the minmod limited solution is still valid for this problem. At  $\tau = 10^4\pi$  the minmod limiter fails to converge at all; this is shown in Fig. 11. The double minmod limiter converges at a second-order rate for both values of  $\tau$

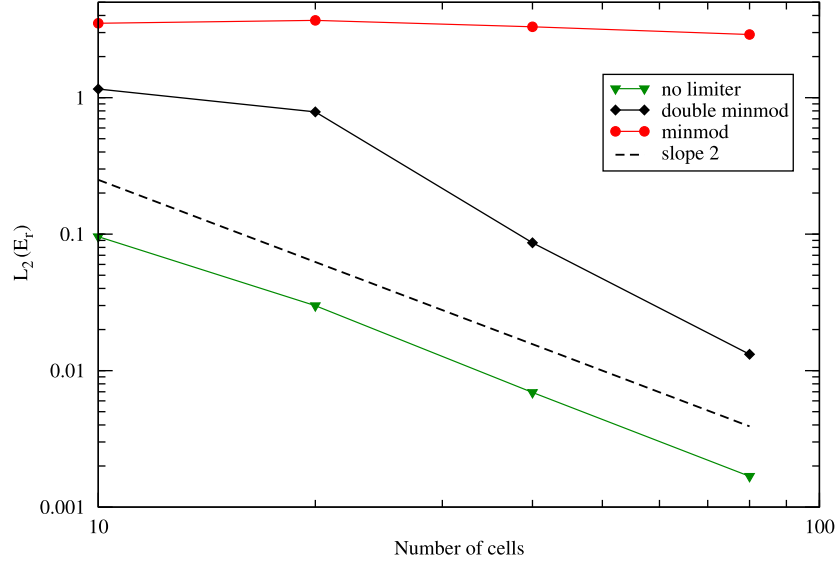


**Fig. 11.** Same as Fig. 10, but with  $\tau = \pi \times 10^4$ , so that problem  $\mathbb{C} = \sigma = (N_x/20) \times 10^5$ .

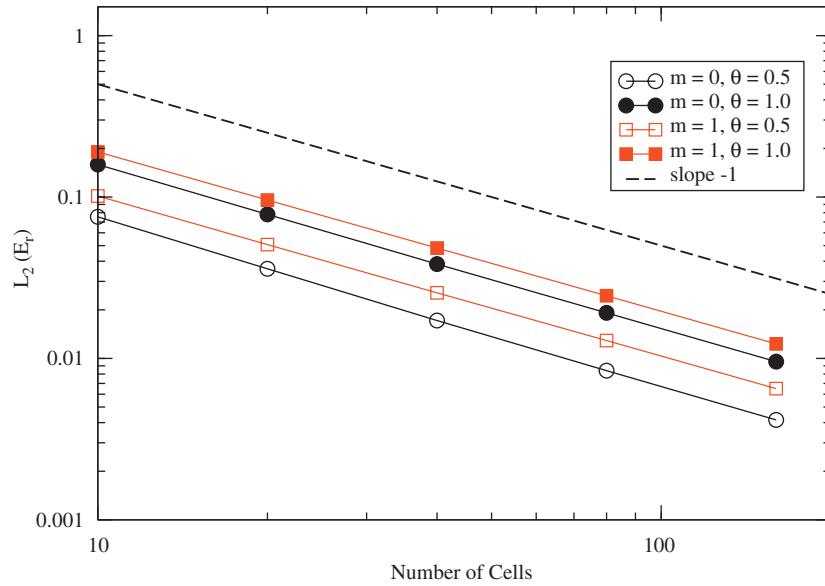


**Fig. 12.** Error between the numerical and analytic solutions for the streaming manufactured solution for varying number of cells with CFL = 0.3,  $\sigma = 1$ , and  $\mathbb{C} = 1000$ .

tested. We do note that the double minmod error is always greater than that from the unlimited solution. The results of Figs. 10 and 11 are consistent with the trends found for radiation transport in Ref. [22].

### 3.2. Streaming results

The results for streaming solution in Fig. 12 show that both the  $m = 0$  and 1 solutions converge to the analytic solution at first order. The results in Fig. 12 were generated with  $A = B = C = 1$ ,  $\alpha = 0.5$ ,  $\sigma = 1$ ,  $\mathbb{C} = 1000$ , and  $\mathbb{P} = 0.1$ ; no slope limiting was used. On the surface this result is surprising, as we would expect to converge at second order. We believe that this result is due to the treatment of the relativistic correction terms in the simulation code. In the current implementation of the simulation code, the relativistic correction terms are lagged at the previous time step in order to avoid a multivariate Newton solve at each time step. This effect was not seen in the diffusion solution because it

evolves on the much slower hydrodynamic time scale, yet the same small time steps were used for its simulations so that spatial errors dominated.

It may also be confusing that for the same value of  $\theta$ , the  $m = 1$  solution has greater error than for  $m = 0$ . This is an example where increasing the order of accuracy in one dimension (in this case  $x$ ) does not mean the overall error is lowered if the discretization in the other dimensions (in this case  $t$ ) are not also improved. If we set  $\sigma = 0$ , so that the first-order accurate treatment of the relativistic correction terms has no effect, then the  $m = 1$  solutions converge at a second-order rate, while the  $m = 0$  solutions converge at a first-order rate.

#### 4. Conclusion

Above, we developed two manufactured solutions for the radiation-hydrodynamics system. We used a grey- $P_1$  radiation transport model and the nonrelativistic Euler equations. One of the solutions is valid in the equilibrium diffusion limit, while the other solution is valid in the limit where radiation streaming dominates. We argued that one should not use the diffusive manufactured solution in the streaming regime, or use the streaming solution in the diffusive regime. Both solutions are needed in order to test a method for radiation hydrodynamics.

We used the equilibrium diffusion solution to test a previously published method. Using the manufactured solution we were able to show that the semi-implicit DG method ( $m = 1$ , LD) preserves the equilibrium diffusion limit when no slope limiter or the double minmod limiter is used. The solution for the step method ( $m = 0$ ) failed in the equilibrium diffusion limit. Finally, for thick enough problems the LD method with the minmod limiter failed to converge to the manufactured solution. These results are consistent with those obtained by Ref. [22] for problems of pure radiation transport (i.e., without hydrodynamic coupling).

Results for the streaming solution converged at first order to the analytic solution for both  $m = 0$  and 1. We conjecture that this result is due to the treatment of the  $v/c$  terms in the numerical method. In future work we will address the issue of how to achieve second-order convergence in the streaming problem.

Demonstrating that a method for the coupled radiation-hydrodynamics equations has a particular convergence rate or verifying a computer code is a difficult task due to the lack of exact or semi-analytic solutions that exist for this system. The solutions above were developed to aid in that task. We believe that these solutions will be useful to test future methods for radiation-hydrodynamics for stability and accuracy. Future work should also include nontrivial boundary conditions in the solution.

#### References

- [1] Coggeshall SV. Analytic solutions of hydrodynamics equations. *Phys Fluids A* 1991;3:757–69.
- [2] Noh WF. Errors for calculations of strong shocks using an artificial viscosity and an artificial heat-flux. *J Comp Phys* 1987;72:78–120.
- [3] Reinicke P, Meyer-ter-Vehn J. The point explosion with heat conduction. *Phys Fluids A* 1991;3:1807–18.
- [4] Su B, Olson GL. Benchmark results for the non-equilibrium Marshak diffusion problem. *JQSRT* 1996;56(3):337–51.
- [5] Su B, Olson GL. An analytic benchmark for non-equilibrium radiative transfer in an isotropically scattering medium. *Ann Nucl Energy* 1997;24(13):1035–55.
- [6] McClarren RG, Hollway JP, Brunner TA. Analytic  $P_1$  solutions for time-dependent, thermal radiative transfer in several geometries. *JQSRT* 2008;109:389–403.
- [7] Olson GL, Auer LH, Hall ML. Diffusion,  $P_1$ , and other approximate forms of radiation transport. *JQSRT* 2000;64:619–34.
- [8] Lowrie RB, Rauenzahn RM. Radiative shock solutions in the equilibrium-diffusion limit. *Shock Waves* 2007;16(6):445–53.
- [9] Lowrie RB, Edwards JD. Radiative shock solutions with grey nonequilibrium diffusion. Technical Report LA-UR-07-6879, Los Alamos National Laboratory, submitted to *Shock Waves*; 2007.
- [10] Lingus C. Analytical test case's [sic] for neutron and radiation transport codes. In: Second conference on transport theory, 1971. p. 655.
- [11] Brunner TA, Mehlhorn T, McClarren RG, Kurecka CJ. Advances in radiation modeling in ALEGRA: a final report for LDRD-67120, efficient implicit multigroup radiation calculations. Technical Report SAND2005-6988, Sandia National Laboratories; November 2005.
- [12] Salari K, Knupp P. Code verification by the method of manufactured solutions. Technical Report SAND2000-1444, Sandia National Laboratories; 2000.
- [13] Roache PJ. Code verification by the method of manufactured solutions. *J Fluids Eng* 2002;124(1):4–10.
- [14] Lowrie RB, Morel JE, Hittinger JA. The coupling of radiation and hydrodynamics. *Astrophys J* 521.
- [15] Larsen EW, Morel JE, Miller WF. Asymptotic solutions of numerical transport problems in optically thick, diffusive regimes. *J Comp Phys* 69(2).
- [16] Larsen EW, Morel JE. Asymptotic solutions of numerical transport problems in optically thick, diffusive regimes II. *J Comp Phys* 1989;83:212–36.
- [17] Larsen EW. The asymptotic diffusion limit of discretized transport problems. *Nucl Sci Eng* 1992;112:336.
- [18] McClarren RG, Holloway JP, Brunner TA. Establishing an asymptotic diffusion limit for Riemann solvers on the time-dependent  $P_N$  equations. In: International topical meeting on mathematics and computation, supercomputing, reactor physics and nuclear and biological applications, American Nuclear Society, Avignon, France, 2005.
- [19] Jin S, Levermore CD. Numerical schemes for hyperbolic conservation laws with stiff relaxation terms. *J Comp Phys* 1996;126:449–67.
- [20] Lowrie RB, Morel JE. Issues with high-resolution Godunov methods for radiation hydrodynamics. *JQSRT* 2001;69:475–89.
- [21] Lowrie RB, Morel JE. Discontinuous Galerkin for hyperbolic systems with stiff relaxation. In: Cockburn B, Karniadakis GE, editors. *Discontinuous Galerkin methods: theory, computation and applications*. Berlin: Springer; 2000. p. 385–90.
- [22] McClarren RG, Lowrie RB. The effects of slope limiting on asymptotic-preserving numerical methods for hyperbolic conservation laws. *J Comp Phys*; July 2008, accepted for publication.
- [23] Drake RP. *High-energy-density physics: fundamentals, inertial fusion, and experimental astrophysics*. Berlin: Springer; 2006.
- [24] Adams ML. Discontinuous finite element transport solutions in thick diffusive problems. *Nucl Sci Eng* 2001;137:298–333.
- [25] Cockburn B, Shu C. The Runge–Kutta local projection  $P^1$ -discontinuous-Galerkin finite element method for scalar conservation laws. *ESAIM Math Modelling Numer Anal* 1991;25:337–61.
- [26] McClarren RG, Evans TM, Lowrie RB, Densmore JD. Semi-implicit time integration for  $P_N$  thermal radiative transfer. *J Comp Phys* 2008;227(16):7561–86.
- [27] Roe PL. Approximate Riemann solvers, parameter vectors, and difference schemes. *J Comp Phys* 1981;43(2):357–72.
- [28] van Leer B. Towards the ultimate conservative difference scheme IV. A new approach to numerical convection. *J Comp Phys* 1977;23(3):276–99.